A HEAT PUMP FOR AUTOMOTIVE APPLICATIONS

Amir Jokar, Mohammad H. Hosni, Steven J. Eckels

Department of Mechanical and Nuclear Engineering
Kansas State University, Manhattan, Kansas, U.S.A.

ABSTRACT

A dual-loop heat pump/air conditioning system for automotive applications is presented in this article. Conventional automotive heating systems have a continuing problem in cold weather due to inadequate thermal energy supply to passenger cabin during the initial engine warm-up. The proposed dual-loop system design may overcome the delayed heating problem, so that the passenger cabin is heated shortly after engine start-up in winter conditions. Furthermore, using special four-way valves makes it possible to switch between heating and cooling modes in the dual-loop system for varying outdoor conditions. Performance of both the system components and the integrated system were tested under various conditions. The thermo-hydrodynamic performance of the heat exchangers within the system was previously analyzed by the coauthors. However, the experimental results and the developed heat transfer and pressure drop correlations are reviewed and presented in this article. For the integrated system, variation of the coefficient of performance versus system variables are analyzed, plotted, and discussed. The results of extensive system testing show that the heat pump coefficient of performance varied from 2 to 5 depending on the outdoor air conditions. It appears that, with system optimization, the proposed dual-loop heating/cooling system would be viable for automotive applications.

Keywords: *automotive heat pump, automotive air conditioning, dual-loop heating/cooling system, secondary fluid loop***.**

1 INTRODUCTION

The automotive dual-loop heating/cooling system used in this study had both a heat pump (HP) mode and an air conditioning (AC) mode. The two modes could be switched for summer or winter conditions using special four-way valves. The integrated system included a standard refrigeration loop consisting of a condenser, an evaporator, a compressor, and an expansion valve using refrigerant R-134a as the working fluid. In addition to the main refrigeration loop, the system had two separate secondary fluid loops using a 50% glycol-water mixture to exchange energy with the refrigeration loop.

The system was operated in heat pump mode during cold seasons, so that the heat rejected from the condenser was used to warm up the passenger cabin through a heater-core while the cold ambient air heated the evaporator. For HP mode, one of the secondary fluid loops was formed between the heater-core and the condenser, and the other one between the external heat exchanger and the evaporator. Part of the engine power was used to run the refrigerant compressor and the glycol-water pumps. Many experiments were conducted to investigate the overall performance of the combined system. An energy balance was applied to the individual components, e.g., the heat exchangers, for each test point to obtain the coefficient of performance (COP) of the system. The COP was defined based on the condenser head load and the compressor mechanical input power. The primary item of interest in this study was the COP of heat pump, thus the secondary loop items were not included. The results showed that COP of the system in HP mode varied between 2 and 5 depending on the outdoor air conditions.

Several studies have used waste thermal energy in an automotive system to run a heat pump within the vehicle. Hamner (1981) investigated the theoretical use of waste heat for automotive air conditioning. Domitrovic et al. (1997) conducted thermodynamic analysis and numerical simulation of an automotive

heat pump system. Antonijevic and Heckt (2004) recently evaluated an automotive heat pump as a supplemental pre-heating system. The researchers built a prototype heat pump system for motor vehicles and tested it under low ambient temperature conditions. The results for the prototype heat pump were analyzed and the system was compared to other heating systems, such as the conventional heating system (using the engine heat rejection) and electrical-heating system. The researchers concluded that the proposed automotive heat pump system had a significantly better cabin-heating performance/fuel consumption ratio than other heating systems.

In this article, the experimental test facilities and test procedure are explained first. The previously developed heat transfer and pressure drop correlations for the heat exchangers within the system are then reviewed and presented. The results for the system test in HP mode, and briefly in AC mode, are finally plotted and discussed.

2 EXPERIMENTAL TEST FACILITIES

A flow diagram of the main refrigeration loop, the two secondary fluid loops, and the two conditioned air loops are shown in Fig. 1.

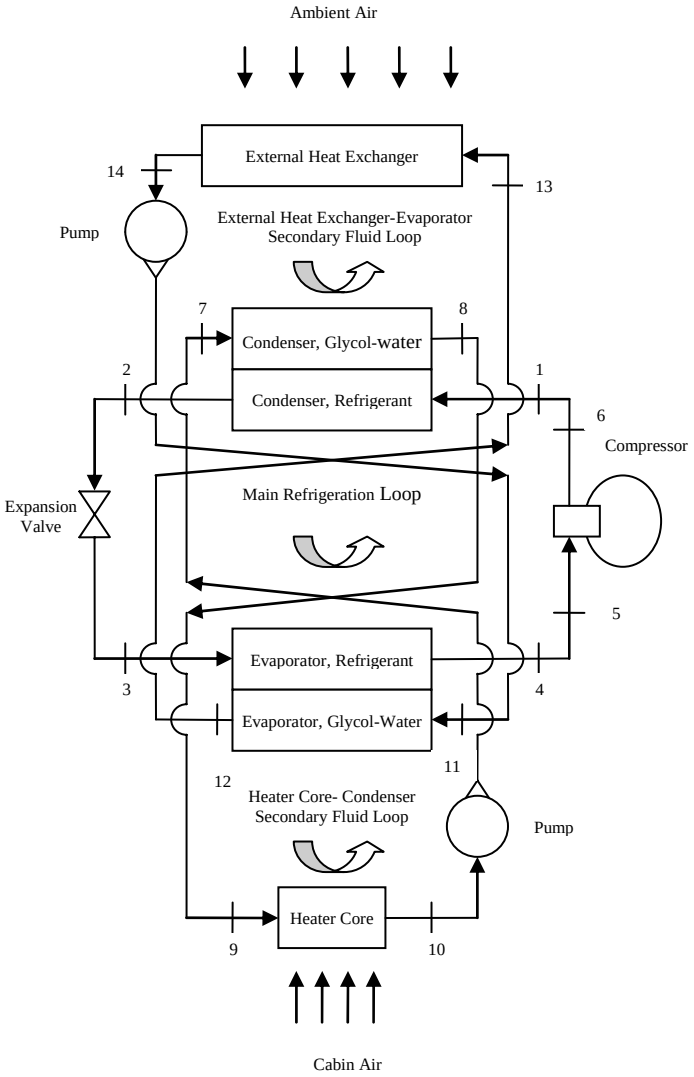

Fig. 1. Flow diagram of the dual-loop heating/cooling system in heat pump mode.

2.1 Refrigeration Loop

The main refrigeration loop included an evaporator, a condenser, a compressor, and an expansion valve. Thermocouples and pressure transducers were installed at the inlet and outlet ports of all components for temperature and pressure measurements. A coriolis-effect flow meter was used to measure the refrigerant mass flow rate, which was controlled by varying the compressor speed using a frequency controlled AC motor. The subcooling at the condenser exit was controlled at a reasonable level greater than zero (around 5 ^{o}C) by varying the refrigerant charge. At the same time, the superheat at the evaporator exit was controlled at the desired level by varying the expansion valve setting.

2.2 Secondary Fluid Loops

Secondary glycol-water mixture loops were designed to exchange energy with the evaporator and the condenser. The temperatures at the inlet/outlet ports of each device were measured using 0.2 m long type-K thermocouples probes. The thermocouple probes were inserted a minimum of 0.1 m into the flow longitudinally and fixed in the center of the 0.02 m inner diameter tubes, so that the bulk temperature could be measured. The pressure drop of the glycol-water mixture passing through the heat exchangers was measured by differential pressure transducers installed between the inlet and outlet ports. The glycol-water mixture flow rates in each loop were measured by a turbine-type flow meter. The connecting pipes and hoses were well insulated to minimize the energy loss through the system.

2.3 Conditioned Air Loops

Two environmental chambers were used in this study. In each chamber, the air temperature and humidity were controlled using conditioned air from external heating/cooling and humidifying/dehumidifying systems. In one of the environmental chambers, conditioned cold air was circulated through the external heat exchanger to simulate winter conditions. In the other chamber, warmer air was circulated through the heater-core to simulate cabin conditions. Two ducts were designed and built for metering air flow through the heater-core and external heat exchanger. An instrumented air flow duct used for circulating cabin air through the heater-core is shown in Fig. 2. The heater-core was installed in the middle of the air duct. An induction fan installed at the duct entrance was used to push conditioned air through the heater-core while a calibrated 0.125 m ASME standard nozzle was used at the duct exit to measure the air flow rate. The mean inlet and outlet air temperatures were measured using several type-K thermocouples distributed on imaginary vertical planes both in the front and back of the heater-core, as shown in Fig. 2.

2.4 Test Procedure

The dual heating/cooling system was set up in HP mode, and a range of test conditions was used to obtain adequate data for analyzing the heat pump performance. All system variables, such as temperatures, pressures, and flow rates, were recorded every 10 seconds as raw data. Once the fluctuations in glycol-water mean temperatures within the system became stable (within ± 1 ^{o}C), the system was considered to be at steady state. Data collection then began and continued for at least 10 minutes for each test condition. The 10-minute averaged data were then used to analyze the system performance.

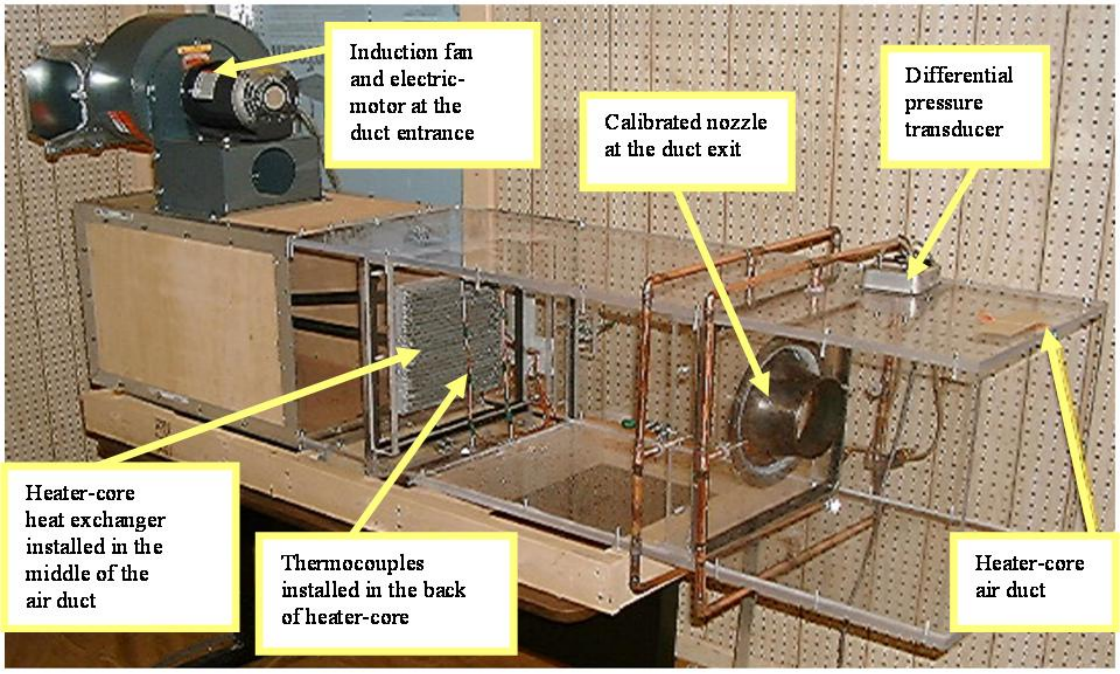

Fig. 2. An instrumented air duct used for circulating cabin air through the heater-core.

3 COMPONENT TEST ANALYSIS

The automotive dual-loop HP/AC system consisted of four heat exchangers installed in the main refrigeration loop or the secondary fluid loops, as shown in Fig. 1. The evaporator and the condenser were a type of brazed plate heat exchangers (BPHEs) with refrigerant R-134a flowing on one side and the glycol-water mixture on the other side. The liquid-air heat exchangers in the secondary fluid loops (i.e., heater-core and external heat exchanger) were a type of minichannel compact heat exchangers. The thermo-hydrodynamic performance of these heat exchangers was analyzed in detail, and the results were reported in Jokar et al. (2004 and 2005). These components are briefly described in this section, and the correlations describing their performance are presented.

3.1 Evaporator and Condenser

Brazed plate heat exchangers (BPHEs) were selected as the evaporator and the condenser of the main refrigeration loop. The BPHEs are a type of plate heat exchangers with corrugated parallel plates that are attached together and fitted into a casing. The parallel plates and the supporting end plates are brazed together in a vacuum furnace. The two neighboring corrugated plates make three-dimensional minichannels that create high turbulent flow and enhance the heat transfer capability per unit volume of heat exchanger. Three different sizes of BPHEs were installed within the system as the evaporator and the condenser to test a variety of configurations. These heat exchangers had the same interior plate design but different numbers of plates (i.e., 34, 40, and 54). The performance of each individual component had to be evaluated to analyze the performance of the integrated system. For this purpose, many tests were done under a wide range of operating conditions to investigate the performance of the BPHEs as the evaporator and the condenser of the refrigeration loop. Heat transfer and pressure drop were then correlated, based on the collected data, for single-phase flow of the glycol-water mixture and two-phase flow of R-134a within the BPHES, as reported in Jokar et al. (2004a, b). The resulting correlations are summarized in Table 1. The hydraulic diameter for the BPHEs was defined as twice the mean plate spacing, and the mass flux was calculated as the total mass flow rate per unit of minimum free-flow open area.

Table 1. Single-phase and two-phase heat transfer and pressure drop correlations within the brazed plate heat exchangers.

Correlation	Heat Transfer	Pressure Drop
Single-Phase Flow (Glycol-Water)	$Nu_{sp} = 0.089\,Re^{p}\,Pr^{n}$ p=0.79 n=0.3 Cooling , n=0.4 Heating 70<Re<900	$C_{f,sp} = 6.431\,Re^{-0.25}$ (70<Re<900)
Evaporation (R-134a)	$Nu_{tp} = 5.653\,Pr_l^{0.333}\,Bo_{eq}^{0.3}\,Re_l^{0.35}\,C_x$ $G_{eq} = GC_x,\ Re_{eq} = Re_l\,C_x,\ Bo_{eq} = Bo/C_x$ $C_x = (1-x_m) + x_m\left(\frac{\rho_l}{\rho_v}\right)^{0.5}$ $Re_{eq} < 3200$	$C_{f,tp} = 3.521\times10^{4}\,Re_l^{-1.35}\,C_x^{-1}$ (Re_{eq}<3200)
Condensation (R-134a)	$Nu_{tp} = 0.0336\,Re_l^{0.622}\,H^{-1}\,Pr_l^{0.33}\left(\rho_l/\rho_v\right)^{0.248}$ $H = \frac{C_p(T_{sat}-T_{wall})}{i_{fg}(1+0.68C_p(T_{sat}-T_{wall})/i_{fg})}$ $Re_l < 1300$	$C_{f,tp} = 2.139\times10^{7}\,Re_{tp}^{-1.6}$ $Re_{tp} = \frac{G.D_h}{\mu_{m,sat}}$ $\frac{1}{\mu_{m,sat}} = \frac{x_m}{\mu_{sup}} + \frac{1-x_m}{\mu_{sub}}$ $Re_{tp} < 4200$

3.2 Heater-Core and External Heat Exchanger

The heater-core and external heat exchanger were components of the two secondary fluid loops. The heater-core was a finned-tube cross-flow heat exchanger used in the heat pump mode to heat the passenger cabin. Air flowed over the finned passages while the glycol-water mixture flowed through the circular tubes. Fin surfaces were parallel continuous thin-plates that were louvered along the air flow passages. These louvers on the fin surfaces promoted turbulence even at low air flow rates. Helical-springs were inserted into the circular tubes to promote turbulent flow and increase heat transfer.

The external heat exchanger was a type of compact heat exchanger similar in design to those used to cool the car engine (radiator). Air flowed over finned passages and the glycol-water mixture flowed through rectangular minichannels. Fin surfaces were louvered to promote turbulence and to reduce the boundary layer thickness of the air flowing across the external heat exchanger to improve its effectiveness. The glycol-water minichannels were equipped with small hemispherical surface enhancements on the top and bottom surfaces to enhance heat transfer rate.

The heat transfer and pressure drop correlations were obtained for the single-phase flow of the glycol-water mixture and air through the heater-core and external heat exchanger, as reported in Jokar et al. (2004c and 2005). The resulting correlations are summarized in Table 2.

The hydraulic diameter for the glycol-water flow in the heater-core was assumed the same as inner circular tube diameter. The hydraulic diameter for the glycol-water flow through the rectangular minichannels of the external heat exchanger was calculated based on the flow cross-sectional area and wetted perimeter. The hydraulic diameter for the air-side, in both heater-core and external heat exchanger, was calculated from the equation defined by Kays and London (1984) for compact heat exchangers.

Table 2. Heat transfer and pressure drop correlations within the heater-core and external heat exchanger.

Correlation	Heat Transfer	Pressure Drop
Heater-Core	$Nu_{sp} = C\,Re^{p}\,Pr^{n}$ $\left[\begin{array}{l} C_g=0.177, C_a=0.268, p_g=0.75, p_a=0.65 \\ n=0.3 \text{ Cooling, } n=0.4 \text{ Heating} \\ 600<Re_g<4600,\ 130<Re_a<750 \end{array}\right]$	$C_{f,g} = 1.654\,Re_g^{-0.2}$ $(600<Re_g<4600)$
External Heat Exchanger	$Nu_{sp} = C\,Re^{p}\,Pr^{n}$ $\left[\begin{array}{l} C_g=0.143, C_a=0.343, p_g=0.70, p_a=0.65 \\ n=0.3 \text{ Cooling, } n=0.4 \text{ Heating} \\ 210<Re_g<700,\ 100<Re_a<580 \end{array}\right]$	$C_{f,g} = 19.21\,Re_g^{-0.8}$ $(210<Re_g<700)$

4 SYSTEM TEST ANALYSIS

Many experiments were conducted to investigate performance of the combined system both in HP and AC modes. For each test point, an energy balance was applied to the components (e.g., condenser, evaporator, and compressor) to obtain COP for the system. The COP was then plotted against different system variables, such as the superheat at the evaporator exit. The goal was to understand how system performance changed with the primary variables of the system. The measured and calculated data for a typical test point in HP mode are summarized in Table 3 at the end of this manuscript. The integrated system analysis is explained for HP mode, and briefly for AC mode, in this section.

4.1 System Test in HP Mode

Several test procedures were used to study performance of the system in HP mode. The variables along with their associated ranges are listed in Table 4.

Table 4. System variables used to evaluate system performance in heat pump mode.

Variable	Variation Range	Compressor Speed
Superheat	8 to 30 ^{o}C	800, 2000 & 3000 rpm
External heat exchanger glycol-water flow rate	300 to 1200 l/h	800, 2000 & 3000 rpm
Heater-core glycol-water flow rate	600 to 1200 l/h	2000 rpm

Typical system curves in HP mode are given in this section for variation of COP versus a) the refrigerant superheat at the evaporator exit and b) the glycol-water flow rate in the secondary fluid loop between the external heat exchanger and the evaporator.

a) COP versus superheat: The refrigerant superheat at the evaporator exit was an important system variable that should be carefully observed and controlled during experiments, especially in HP mode. Fluctuations of system temperatures (e.g., the superheated vapor at the evaporator exit) in HP mode were larger than in AC mode. Although the glycol-water temperatures were stable within ± 1 ^{o}C, the refrigerant superheated vapor temperature tended to vary more (± 3 ^{o}C) but with a uniform and steady oscillation. The fluctuation of temperatures even increased when the compressor was run at low speeds. For the tests reported herein, the superheat was varied from 8 to 30 ^{o}C for the three different compressor speeds used.

Figure 3 shows a plot of COP versus the refrigerant superheat at the evaporator exit in HP mode. This figure shows that COP decreased with increased superheat at low compressor speeds, while it was nearly constant at higher speeds. To better understand the variation of COP with the superheat (Fig. 3), the system low side pressure at the compressor inlet and high side pressure at the compressor outlet were investigated. The pressures are plotted versus the superheat in Fig. 4 for the three compressor speeds. For

each test point, the closer the high and low side pressures were the less input power was needed by the compressor. Less input power had a positive effect on the heat pump performance as it improves COP.

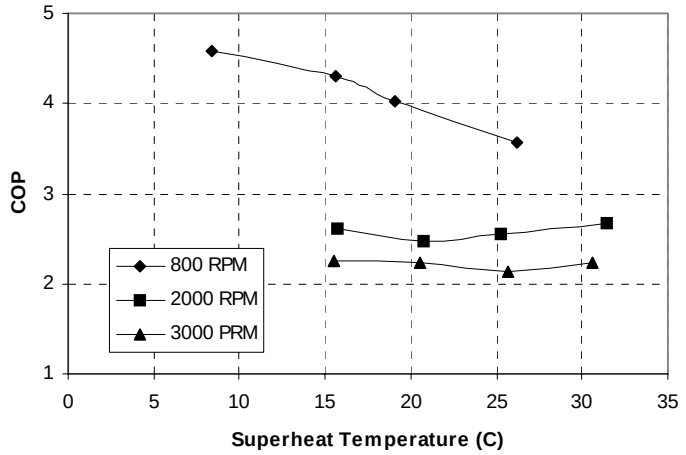

Fig. 3. Variations of the coefficient of performance versus the refrigerant superheat at the evaporator exit for different compressor speeds in heat pump mode.

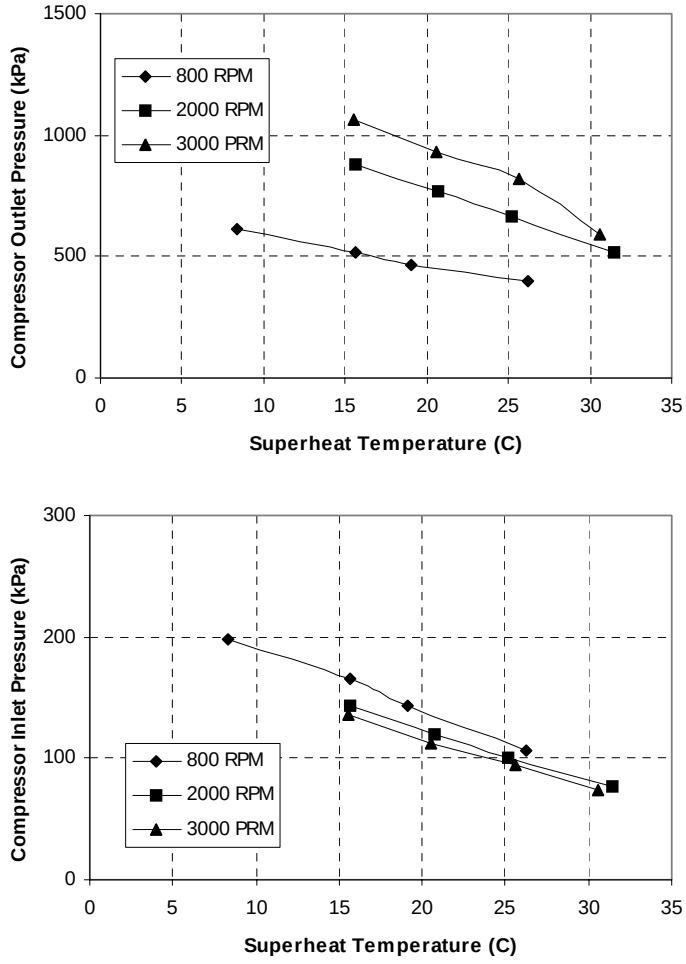

Fig. 4. Variations of the system low and high side pressures versus the refrigerant superheat at the evaporator exit for different compressor speeds in heat pump mode.

The plots in Fig. 4 show that the low side pressure decreased with increasing superheat for all compressor speeds, causing both the evaporator heat transfer rate and COP to decrease. However, the high side pressure also decreased, as seen in Fig. 4, causing the condenser heat transfer rate to decrease but COP to increase. Considering these two effects, the results showed that the required compressor power decreased slightly, especially at higher compressor speeds, causing COP to increase. On the other hand, decreasing the heat transfer rate in the condenser caused COP to decrease. The results of superimposing these effects on the system performance are plotted in Fig. 3. Measured and calculated data for a typical test point at the compressor speed of 2000 rpm is summarized in Table 3.

b) COP versus glycol-water flow rate: Changing the glycol-water flow rates within the secondary fluid loops was another point of interest in evaluating the heat pump performance. In a test procedure, the glycol-water flow rate in the evaporator was changed from 300 to 1200 l/h at three compressor speeds holding all other system parameters constant. Figure 5 shows a plot of COP versus the glycol-water flow rate within the secondary fluid loop between the external heat exchanger and the evaporator.

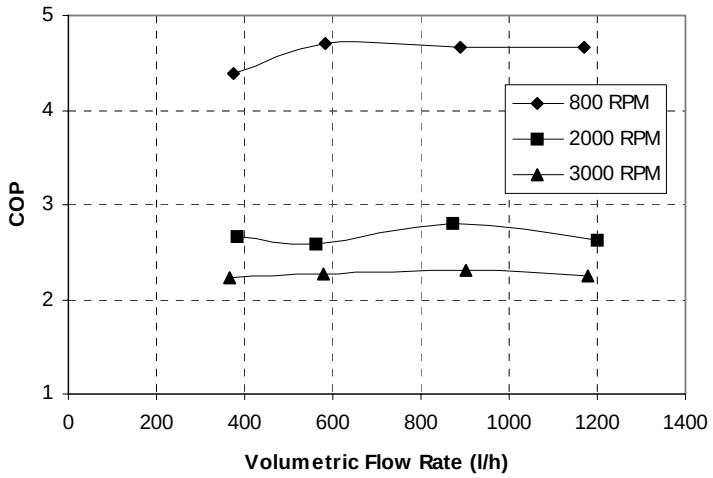

Fig. 5. Variations of the coefficient of performance versus the glycol-water flow rate within the secondary fluid loop between the external heat exchanger and the evaporator in heat pump mode.

Figure 5 shows that COP did not vary significantly as the glycol-water flow rate changed in the evaporator. However, circulating more glycol-water in the secondary fluid loop increased the Reynolds number both in the external heat exchanger and the evaporator. Similar curves were observed for the variations of COP versus the glycol-water flow rate in the secondary fluid loop between the heater-core and the condenser. These results can be explained by the variations of heat transfer rates in the evaporator and the condenser for these tests. The evaporator heat transfer rate increased as the glycol-water flow rate increased, especially at higher compressor speeds. In fact, increasing the glycol-water flow rate caused the Reynolds number and, as a result, the evaporator heat transfer coefficient to increase. An energy balance on the system components showed that the heat transfer rate in the condenser also increased, and thus more heat was rejected from the condenser to the heater-core. Superposing two effects causes COP in Fig. 5 to stay nearly constant with increased glycol-water flow rate. This means that more thermal energy is transferred to the cabin without affecting COP significantly.

An uncertainty analysis of COP showed that the average uncertainty for the experimental data taken in HP mode was about 8% for most of the experiments. A few conditions in the test matrix caused ice to form over the external heat exchanger and cover part of its frontal surface area. For these conditions, digital photography from back of the external heat exchanger was used to document the ice build up. Note that this does not affect the calculation of COP presented in this section.

4.2 System Test in AC Mode

The dual-loop heating/cooling system was also studied in AC mode, and variations of COP were investigated versus different system variables. These variables along with their associated ranges are listed in Table 5.

Table 5. System variables used to evaluate system performance in air conditioning mode.

Variable	Variation Range
External heat exchanger inlet air velocity	1 to 4 m/s
External heat exchanger inlet air temperature	20 to 50 ^{o}C
External heat exchanger glycol-water flow rate	600 to 1500 l/h
Cooler-core inlet air relative humidity	10 to 50%
Cooler-core inlet air temperature	20 to 50 ^{o}C
Cooler-core inlet air mass flow rate	200 to 650 kg/hr
Cooler-core glycol-water flow rate	600 to 1300 l/h
Evaporator outlet refrigerant superheat	6 to 17 ^{o}C
Compressor speed	1000 to 3000 rpm

For AC mode, one of the secondary fluid loops was formed between the external heat exchanger and the condenser, and the other one between the cooler-core and the evaporator. A typical system curve in AC mode is given in this section for the variation of COP with the compressor speed. In this test procedure, the compressor speed was changed from 1000 to 3000 rpm to investigate the effect of this variable on performance of the system in AC mode. The compressor speed was maintained at 3000 rpm for the other 8 test conditions presented in Table 5. The variation of COP versus compressor speed in AC mode is shown in Fig. 6.

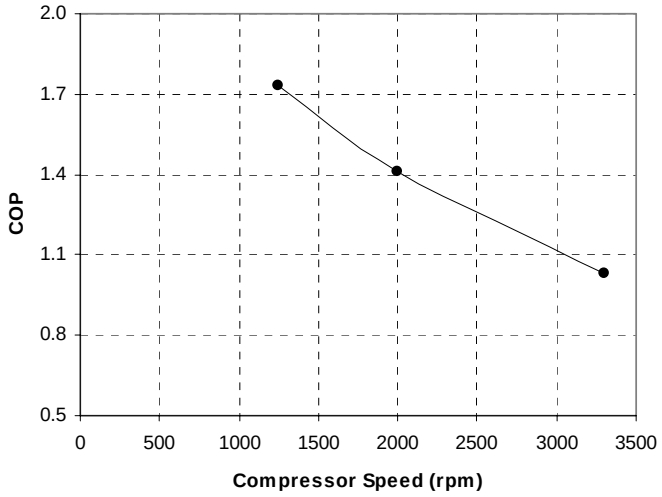

Fig. 6. Variations of the coefficient of performance versus the compressor speed in air conditioning mode.

It appears from Fig. 6 that as the compressor speed increased, COP decreased. This behavior could be predicted since increasing the compressor speed causes the input power to increase. The increase in compressor speed also caused the system low and high side pressures to diverge from each other, as shown in Fig. 7.

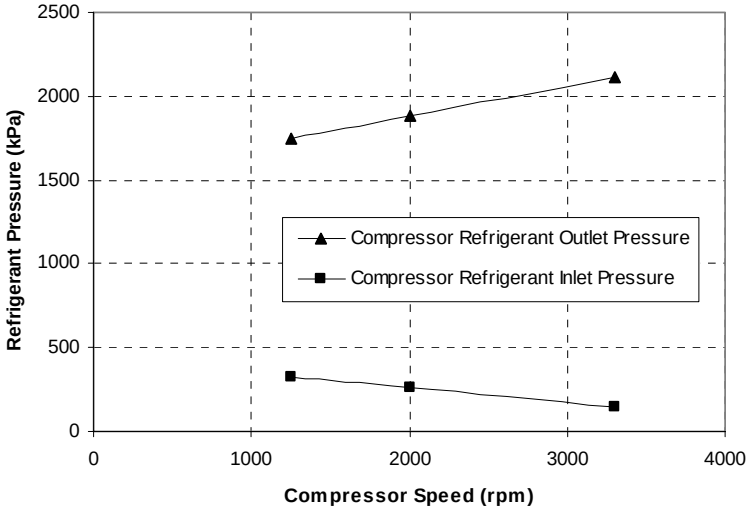

Fig. 7. Variations of the system low and high side pressures versus the compressor speed in air conditioning mode.

The divergence of low and high side pressures, as shown in Fig. 7, led to decreased COP. The results showed that the evaporator heat transfer rate stayed nearly constant in this experiment while the condenser heat transfer rate increased noticeably. The net cycle heat transfer rate thus increased, as did the net cycle input power. The results of this experiment showed that it was more beneficial to decrease the compressor speed when the cooling load of the cooler-core was low. The system performance may be optimized using a self-controlled variable speed compressor.

5 SUMMARY AND CONCLUSIONS

A dual-loop heating/cooling system was studied in both heat pump (HP) and air conditioning (AC) modes. Many experiments were conducted to investigate the performance of the combined system. In each experiment, the variation of the coefficient of performance (COP) versus system variables was analyzed for different conditions. The COP for the heat pump cycle ranged from 2 to 5. The proposed automotive dual-loop HP/AC system may have several advantages over the conventional separated heating and cooling systems: 1) the integrated dual-loop HP/AC system is more compact and needs fewer components, 2) the delayed heating problem during the cold seasons is almost resolved, and the passenger cabin is warmed right after the engine start-up, and 3) adequate thermal energy is supplied to the cabin especially for those cars without sufficient waste thermal energy to warm the cabin in cold conditions (the new direct injection engines). The system has also some disadvantages: 1) it may increase engine emissions due to increased load from compressor operation, and 2) the engine fuel consumption may increase slightly. The results of this experimental study may be used to design an integrated HP/AC system. They can also serves as a source for validation of numerical simulation models.

REFERENCES

Antonijevic D. and R. Heckt, 2004. “Heat pump supplemental heating system for motor vehicles,” *Proceedings of the Institution of Mechanical Engineers, Part D: Journal of Automobile Engineering,* Vol. 218, No. 10, pp. 1111-1115.

Domitrovic R. E., V. C. Mei, and F.C. Chen 1997. “Simulation of an automotive heat pump,” *ASHRAE Transactions,* Vol. 103, Part 2, pp. 291-296.

Hamner R. M. 1981. “Use of waste heat for automotive air conditioning,” *SAE Preprints*, No. 810504.

Jokar A., S. J. Eckels, M. H. Hosni, and T. P. Gielda 2004a. ”Condensation heat transfer and pressure drop of the brazed plate heat exchangers using R-134a,” *Journal of Enhanced Heat Transfer,* Vol.11, No 2, pp. 161-182.

Jokar A., S. J. Eckels, and M. H. Hosni 2004b. “Thermo-hydrodynamic of the evaporation of refrigerant R-134a in brazed plate heat exchangers,” *Proceedings of the 2004 ASME Heat Transfer/Fluids Engineering Summer Conference,* HT-FED04-56573, Charlotte, NC, USA.

Jokar A., S. J. Eckels, and M. H. Hosni 2004c. “Evaluation of heat transfer and pressure drop for the heater-core in an automotive heat pump system,” *Proceedings of the 2004 ASME International Mechanical Engineering Congress and RD&D Expo,* IMECE2004-60824, Anaheim, CA, USA.

Jokar A., M. H. Hosni, and S. J. Eckels 2005. “Heat transfer and pressure drop characteristics for the rectangular minichannel heat exchanger in an automotive air conditioning system,” *Proceedings of the 2005 ASME Heat Transfer Summer Conference*,” HT2005-72061, San Francisco, CA, USA.

Kays W. M. and A. L. London. 1984. *Compact Heat Exchangers*, 3rd Ed., McGraw-Hill, New York.

ACKNOWLEDGEMENTS

This study was supported through a research grant from Visteon, Inc. The coauthors acknowledge Dr. Thomas P. Gielda for his technical support and coordination during the experimental phase of the project.

NOMENCLATURE

Bo: boiling number
C: constant
C_p: specific heat capacity (J/kg. K)
C_f: Fanning friction factor
C_x: coefficient (for vapor quality)
D: diameter (m)
G: mass flux (kg/m^2.s)
H: dimensionless parameter
i: enthalpy (J/kg)
n: Prandtl number exponent
Nu: Nusselt number
p: Reynols number exponent
Pr: Prandtl number
Re: Reynolds number
T: temperature (K)
x: vapor quality

Greek Symbols:

μ: dynamic viscosity (Pa.s)
ρ: density (kg/m^3)

Subscripts:

a: air
eq: equivalent
fg: liquid-vapor
g: glycol-water mixture
h: hydraulic
l: liquid
m: mean value
r: refrigerant (R-134a)
sat: saturation
sp: single-phase
sub: subcooled
sup: superheated
tp: two-phase
v: vapor
wall: tube/channel wall

Table 3. Variations of refrigerant superheat at the evaporator exit at the compressor speed of 2000 rpm for the system test in heat pump mode.

Variable	Unit	T_{sup} (2000 RPM)			
		15 °C	***20 °C***	***25 °C***	***31 °C***
Inputs					
External heat exchanger inlet air velocity	(m/s)	1.9	1.5	1.4	1.0
External heat exchanger inlet air temperature	(°C)	10.1	9.7	9.5	8.9
Compressor speed	(RPM)	2000	2000	2000	2000
Heater-core inlet air mass flow rate	(kg/h)	477	471	469	480
Heater-core inlet air relative humidity	(%)	77	71	70	74
Heater-core inlet air temperature	(°C)	-18.38	-18.03	-18.10	-17.83
External heat exchanger glycol-water volumetric flow rate	(l/h)	1186	1188	1193	1181
Heater-core glycol-water volumetric flow rate	(l/h)	1200	1195	1191	1192
Evaporator outlet refrigerant superheat	(°C)	15.7	20.7	25.2	31.5
Measurements					
Condenser outlet refrigerant subcooling	(°C)	5.8	5.9	5.4	3.9
Ambient air temperature	(°C)	10.1	9.7	9.5	8.9
Ambient air pressure	(kPa)	97.5	97.5	97.5	97.3
External heat exchanger outlet air temperature	(°C)	1.4	3.1	3.8	3.0
Heater-core outlet air temperature	(°C)	17.3	13.9	10.5	3.9
Heater-core outlet air relative humidity	(%)	5.6	6.6	8.2	13.8
Refrigerant mass flow rate in the main refrigeration loop	(kg/s)	0.022	0.018	0.015	0.011
Compressor inlet refrigerant pressure	(kPa)	143.3	119.2	100.9	77.4
Compressor outlet refrigerant pressure	(kPa)	878.4	767.1	668.5	516.2
Condenser inlet refrigerant pressure	(kPa)	887.0	779.5	683.3	525.1
Condenser outlet refrigerant pressure	(kPa)	884.5	777.1	680.6	523.5
Evaporator inlet refrigerant pressure	(kPa)	162.4	132.5	110.6	85.1
Evaporator outlet refrigerant pressure	(kPa)	162.6	132.8	110.9	83.7

Table 3 continued

Variable	Unit	T_{sup} (2000 RPM)			
		15 °C	***20 °C***	***25 °C***	***31 °C***
Measurements					
Compressor inlet refrigerant temperature	(°C)	0.5	1.2	1.7	2.4
Compressor outlet refrigerant temperature	(°C)	99.3	102.8	105.5	106.7
Condenser inlet refrigerant temperature	(°C)	95.8	98.0	99.3	99.5
Condenser outlet refrigerant temperature	(°C)	29.1	24.4	20.4	13.2
Evaporator inlet refrigerant temperature	(°C)	-15.2	-20.0	-24.1	-29.8
Evaporator outlet refrigerant temperature	(°C)	0.5	0.7	1.2	1.3
Evaporator inlet glycol-water temperature	(°C)	-0.4	-0.3	0.1	0.1
Evaporator outlet glycol-water temperature	(°C)	-4.0	-3.4	-2.5	-2.0
Condenser inlet glycol-water temperature	(°C)	27.7	23.8	20.0	12.9
Condenser outlet glycol-water temperature	(°C)	32.7	28.2	23.8	16.0
Heater-core inlet air temperature	(°C)	-18.4	-18.0	-18.1	-17.8
Heater-core outlet air temperature	(°C)	17.3	13.9	10.5	3.9
External heat exchanger inlet air temperature	(°C)	10.1	9.7	9.5	8.9
External heat exchanger outlet air temperature	(°C)	1.4	3.1	3.8	3.0
Calculations					
Condenser refrigerant heat transfer rate	(W)	5329	4475	3790	2911
Condenser glycol-water heat transfer rate	(W)	5916	5083	4404	3615
Evaporator refrigerant heat transfer rate	(W)	3602	3038	2588	2017
Evaporator glycol-water heat transfer rate	(W)	4146	3473	2971	2277
Heater-core air heat transfer rate	(W)	4753	4209	3754	2920
Heater-core glycol-water heat transfer rate	(W)	5376	4796	4339	3533
External heat exchanger air heat transfer rate	(W)	4001	2505	1944	1409
External heat exchanger glycol-water heat transfer rate	(W)	3692	3056	2572	1812
Compressor mechanical power	(W)	2264	2048	1722	1355
Compressor torque	(N.m)	10.81	9.78	8.22	6.47
System coefficient of performance		2.61	2.48	2.56	2.67
Additional Data					
Heater-core inlet glycol-water temperature	(°C)	31.9	27.5	23.2	15.4
Heater-core outlet glycol-water temperature	(°C)	27.3	23.4	19.5	12.4
External heat exchanger inlet glycol-water temperature	(°C)	-3.6	-3.0	-2.1	-1.6
External heat exchanger outlet glycol-water temperature	(°C)	-0.4	-0.3	0.1	0.0
Heater-core glycol-water pressure drop	(kPa)	21.4	21.7	21.7	23.1
External heat exchanger glycol-water pressure drop	(kPa)	21.5	21.5	21.1	19.6
Evaporator glycol-water pressure drop	(kPa)	4.1	4.2	4.0	4.0
Condenser glycol-water pressure drop	(kPa)	4.0	3.7	4.0	3.8
Evaporator refrigerant pressure drop	(kPa)	-0.2	-0.4	-0.4	1.4
Condenser refrigerant pressure drop	(kPa)	2.5	2.3	2.6	1.6
Evaporator inlet refrigerant vapor quality	(%)	28.9	28.2	27.6	26.0